Evidence for Chiral Wobbler in Nuclei

R. J. Guo (郭睿巨),[1] S. Y. Wang (王守宇),[1,*] C. Liu (刘晨),[1] R. A. Bark,[2] J. Meng (孟杰),[3,4,5] S. Q. Zhang (张双全),[3]
B. Qi (亓斌),[1] A. Rohilla,[1] Z. H. Li (李智焕),[3] H. Hua (华辉),[3] Q. B. Chen (陈启博),[6] H. Jia (贾慧),[1] X. Lu (陆晓),[1]
S. Wang (王硕),[1] D. P. Sun (孙大鹏),[1] X. C. Han (韩星池),[1] W. Z. Xu (许文政),[1] E. H. Wang (王恩宏),[1]
H. F. Bai (白洪斐),[1] M. Li (李淼),[1] P. Jones,[2] J. F. Sharpey-Schafer,[2,7] M. Wiedeking,[2,8] O. Shirinda,[2,5,9] C. P. Brits,[2,5]
K. L. Malatji,[2,5] T. Dinoko,[2] J. Ndayishimye,[2] S. Mthembu,[2,10] S. Jongile,[2,5] K. Sowazi,[2,7] S. Kutlwano,[2] T. D. Bucher,[2,5]
D. G. Roux,[11] A. A. Netshiya,[2,7] L. Mdletshe,[2,10] S. Noncolela,[7] and W. Mtshali[10]

[1]*Shandong Provincial Key Laboratory of Optical Astronomy and Solar-Terrestrial Environment,*
School of Space Science and Physics, Institute of Space Sciences, Shandong University,
Weihai 264209, People's Republic of China
[2]*iThemba LABS, 7129 Somerset West, South Africa*
[3]*School of Physics and State Key Laboratory of Nuclear Physics and Technology, Peking University,*
Beijing 100871, People's Republic of China
[4]*School of Physics and Nuclear Energy Engineering, Beihang University, Beijing 100191, People's Republic of China*
[5]*Department of Physics, University of Stellenbosch, Matieland 7602, South Africa*
[6]*Department of Physics, East China Normal University, Shanghai 200241, People's Republic of China*
[7]*Department of Physics, University of the Western Cape, P/B X17 Bellville 7535, South Africa*
[8]*School of Physics, University of the Witwatersrand, Johannesburg 2050, South Africa*
[9]*Department of Physical and Earth Sciences, Sol Plaatje University, Private Bag X5008, Kimberley 8301, South Africa*
[10]*Department of Physics, University of Zululand, Private Bag X1001, KwaDlangezwa 3886, South Africa*
[11]*Department of Physics and Electronics, Rhodes University, Grahamstown 6410, South Africa*

(Received 24 November 2022; accepted 30 January 2024; published 28 February 2024)

Three $\Delta I = 1$ bands with the $\pi g_{9/2} \otimes \nu g_{9/2}$ configuration have been identified in $^{74}_{35}\mathrm{Br}_{39}$. Angular distribution, linear polarization, and lifetime measurements were performed to determine the multipolarity, type, mixing ratio, and absolute transition probability of the transitions. By comparing these experimental observations with the corresponding fingerprints and the quantum particle rotor model calculations, the second and third lowest bands are, respectively, suggested as the chiral partner and one-phonon wobbling excitation built on the yrast band. The evidence indicates the first chiral wobbler in nuclei.

DOI: 10.1103/PhysRevLett.132.092501

Shape is one of the most fundamental properties for nuclei, since it is a manifestation of the self-organization of a finite fermionic system. Atomic nuclei generally exhibit spheroidal shape or axially symmetric shapes that deviate from the sphere. The loss of axial symmetry could involve triaxial deformation. The question of whether stable triaxial shapes exist in nuclei has been debated for decades. Until 2001, the discovery of nuclear chirality [1] and the wobbling mode [2] had provided direct evidence for the stable triaxial deformation in nuclei.

The existence of chirality in atomic nuclei was initially suggested by Frauendorf and Meng [3]. Chiral symmetry breaking manifests itself in the appearance of a pair of $\Delta I = 1$ doublet bands with the same parity, which are called chiral doublet bands [3]. Several fingerprints for ideal chiral doublet bands [3–7] are suggested as follows: (i) nearly degenerate in excitation energies, (ii) smooth dependence of energy staggering parameters $S(I)$ with spin, (iii) similar spin alignments, (iv) similar $B(E2)$ and $B(M1)$ values, (v) the odd-even staggering of $B(M1)$ values and opposite phase for in-band and interband transitions, and (vi) the vanishing of the interband $E2$ transitions at high spin.

The wobbling mode in nuclei was predicted in the 1970s in analogy to the rotating asymmetrical top [8]. It occurs when the core angular momentum wobbles about the principal axis with the largest moment of inertia in triaxial nuclei. These conditions may give rise to sequences of rotational bands with successive excitations of wobbling phonons, $n_w = 0, 1, 2, \ldots$. The known fingerprints of the wobbling bands [2,8–11] are that the $n_w = 0$ and 1 bands exhibit similar moments of inertia, spin alignments, and $B(E2; I \to I-2)$ values. In addition, the interband $\Delta I = 1$ transitions are dominated by the $E2$ component.

In the past two decades, chirality and the wobbling mode were established in a few mass regions of the nuclear chart. Candidate chiral doublet bands were reported experimentally in the $A \approx 80$, 100, 130, and 190 mass regions (see reviews [7,12–19] and references therein). In addition, wobbling bands were reported in the $A \approx 110$ [20,21], 130 [22–27], 160 [2,9,28–31], and 190 [32,33] mass regions. However, whether chirality and the wobbling mode can coexist in a single nucleus is still an open question. On the theoretical side, chiral wobblers in nuclei were first suggested in the quantum particle rotor model (PRM) by analyzing angular momentum components [34]. Recently, further analyses of mixing ratios have been performed to study the possible wobbling motion in multiple chiral doublets [35]. In this Letter, we report the evidence for the first coexistence of the chiral and wobbling modes with the same configuration (chiral wobbler) in nuclei. The present observations also provide the first example of a wobbling band in odd-odd nuclei and open up a new mass region where the wobbling mode is established.

Medium- and high-spin states in ^{74}Br were populated using the ^{58}Ni(^{19}F, $2p1n$) reaction at a beam energy of 62 MeV. A target consisting of 1.0 mg/cm^2 of highly enriched ^{58}Ni evaporated onto a 12.8 mg/cm^2 Au backing was used in the experiment. The thickness of the backing was chosen such that the recoil nuclei are completely stopped in the backing, thus enabling the determination of level lifetimes using the Doppler-shift-attenuation method. The emitted γ rays were detected by the detector array AFRODITE [36,37] equipped with eight Compton suppressed clover detectors (five at 90° and three at 135° relative to the beam direction). In the experiment, about 3.5×10^9 γ-γ coincidence events were collected. The coincidence events were sorted off-line into a symmetric and several asymmetric matrices as well as a γ-γ-γ coincidence cube. The symmetric matrix and cube were used to construct the level scheme. The asymmetric matrices were used to extract the angular distribution from oriented state (ADO) ratios [38], linear polarization values [39,40], and level lifetimes.

A partial level scheme for ^{74}Br relevant to the focus of this Letter is presented in Fig. 1, with three bands labeled as $B1$–$B3$. Three new transitions have been added to band 1. Bands 2 and 3 have been extended to complete $\Delta I = 1$ bands by adding several new transitions. Many new transitions linking bands 2 and 3 to band 1 are also identified. These new transitions can be seen in Fig. 2, which shows representative gated spectra supporting the present level scheme. The spin and parity assignments of the states were deduced by the measured ADO ratios and linear polarizations. To obtain the $E2/M1$ mixing ratio (δ) of transitions, the ADO ratios and linear polarizations of the transitions were compared with the corresponding theoretical values [41–44]. Several representative comparisons are shown in Fig. 3.

Lifetimes of the excited states were determined from Doppler shifts of γ rays observed in coincidence spectra at 135° and 90° detectors, respectively. Gates were placed on the transitions below the considered ones because of having better statistics and resulted in smaller uncertainties compared to those of gating above. The level lifetimes were extracted using a modified LINESHAPE package [47]. Electronic stopping powers were taken from Ziegler's tabulation [48] with low-energy modifications. Side feeding into each level and feeding into the topmost level of each band was modeled by a five-state rotational cascade. These feeding intensities and times together with the lifetime, background, and contaminant peak(s) were input to the line shape analysis as independent variable parameters. The simulated line shape was then calculated using the parameters and fitted to the experimental spectra using χ^2 minimization. Details of the fitting procedure can be found in Refs. [47,49,50]. Examples of the line shape analyses are shown in Fig. 4, and the extracted lifetimes are compared with the previously measured ones [51–53] in Table I. As shown in Table I, the present lifetimes agree with the previous ones within the errors.

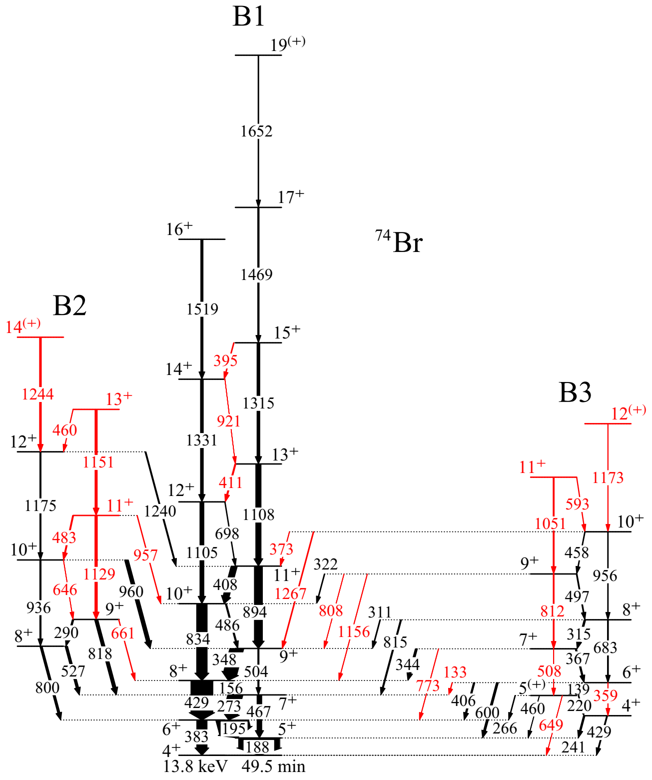

FIG. 1. Partial level scheme for ^{74}Br from the present Letter. All the observed transitions eventually feed into the 4^+ isomer at 13.8 keV [45,46]. New transitions and levels are marked as red. The transition width represents intensities. Intensities are normalized to 383 keV transition as 100.

Band 1 has already been assigned the $\pi g_{9/2} \otimes \nu g_{9/2}$ configuration [45,53,54]. As shown in Fig. 1, the existence of numerous strong linking transitions between bands 1 and 2 and 1 and 3 implies that bands 2 and 3 have the same $\pi g_{9/2} \otimes \nu g_{9/2}$ configuration as band 1, as discussed in Refs. [1,55,56]. This is further supported by the similar alignment and kinematic moments of inertia of the bands 1–3 shown in Fig. 5.

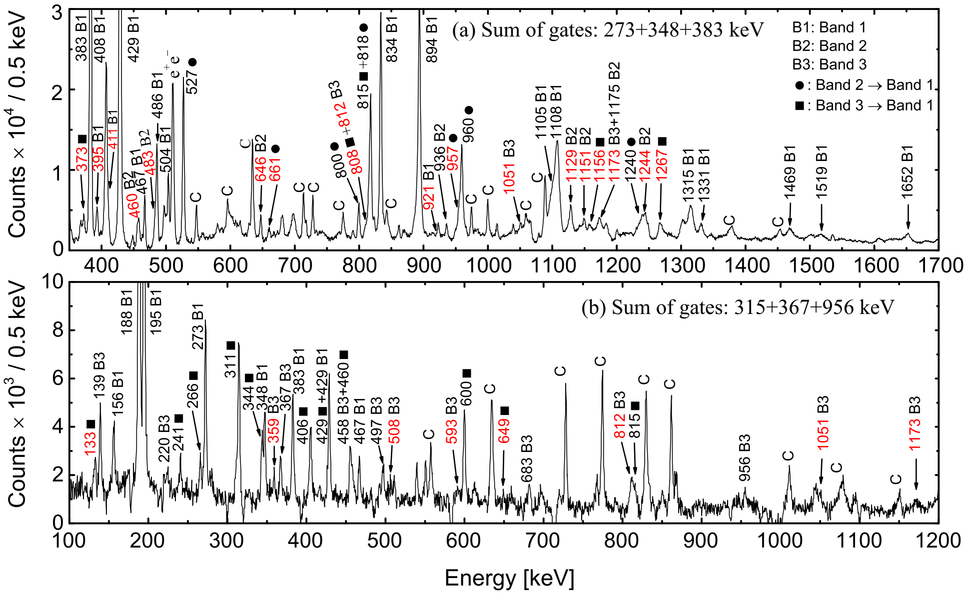

FIG. 2. The γ-ray coincidence spectra gated on the (a) 273 + 348 + 383 keV transitions and (b) 315 + 367 + 956 keV transitions in ^{74}Br. The peaks labeled C indicate contaminations. New transitions are marked as red.

In the neighboring isotopes ^{76,78,80,82}Br, the yrast and second lowest bands based on the $\pi g_{9/2} \otimes \nu g_{9/2}$ configuration were interpreted as chiral doublet bands [57–60]. To investigate whether bands 1 and 2 in ^{74}Br are also associated with chirality, we compared the experimental character of bands 1 and 2 with the fingerprints of chiral doublet bands. The excitation energies $E(I)$, energy staggering parameters $S(I) = [E(I) - E(I-1)]/2I$ and absolute transition probabilities $B(E2)$ and $B(M1)$ for bands 1–3 as well as the $B(M1)$ and $E2$ fractions for interband $\Delta I = 1$ transitions between bands 1 and 2 and 1 and 3 are plotted in the left column of Fig. 6 (see Supplemental Material for numerical details [61]). As shown in Fig. 6, the energy differences of bands 1 and 2 are similar to those of chiral doublet bands in ^{76,78,80,82}Br. Furthermore, the $S(I)$ of bands 1 and 2 shows a smooth variation as a function of spin. The two bands also have similar i_x (see Fig. 5), in-band $B(E2)$, and in-band $B(M1)$ values. The $B(M1)$ values exhibit odd-even staggering and the opposite phase of the staggering for the in-band and interband $\Delta I = 1$ transitions. In the high-spin regime, there are no obvious peaks at possible interband $\Delta I = 2$ $E2$ transition energies in the Supplemental Material figure [61]. Finally, as can be seen in Fig. 6, the interband $\Delta I = 1$ transitions between bands 1 and 2 are dominated by $M1$ components. In short, these experimental features fulfill all the fingerprints of chiral doublet bands, which indicates that bands 1 and 2 are a pair of chiral doublet bands.

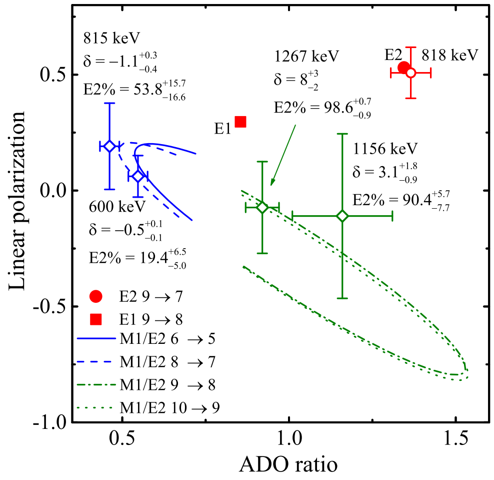

FIG. 3. Examples of experimental (open symbols with bars) and calculated (solid square, circle, as well as solid, dashed, dot-dashed, and dotted lines) ADO ratios and linear polarization values for the representative linking transitions between bands 1 and 3, and for a known $E2$ transition between bands 1 and 2. The mixing ratio value varies from −0.2 (lower end) to −5.1 (upper end), for the solid and dashed lines, and varies from 0.0 (lower end) to 11.4 (upper end), for the dot-dashed and dotted lines.

Band 3 has similar i_x, $J^{(1)}$ (see Fig. 5), $S(I)$, and in-band $B(E2)$ values (see Fig. 6) to band 1, but one can see in Fig. 6 that the in-band $B(M1)$ values of band 3 have an opposite staggering phase compared to band 1, making band 3 different from the chiral partner. More importantly, the $E2$ fractions of the interband $\Delta I = 1$ transitions between bands 1 and 3 increase with spin and reach 90% at high spin, which are significantly larger than that of the other transitions in the present level scheme. These experimental features imply that the even and odd spin sequences of band 3 originate from one-phonon wobbling excitations of the odd and even spin sequences of band 1,

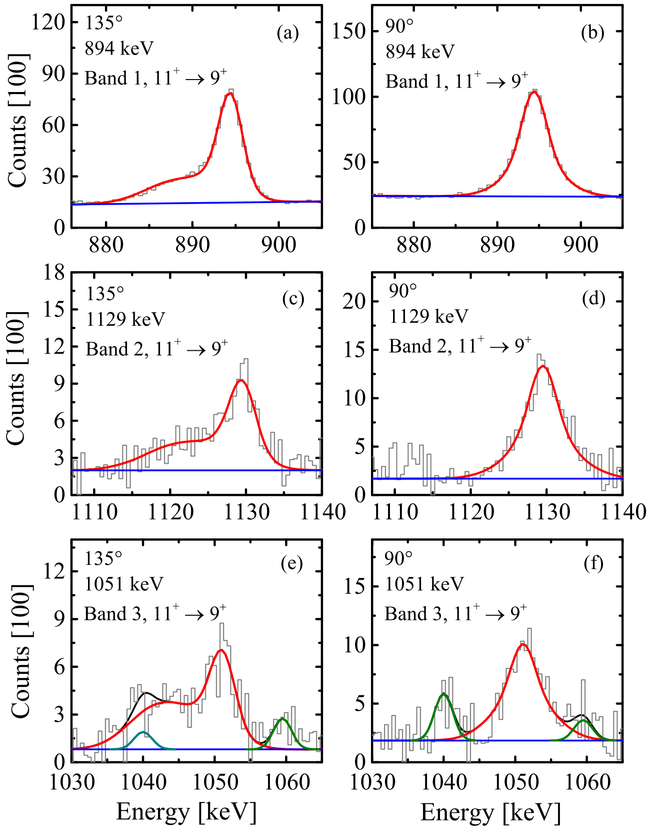

FIG. 4. Line shape fits to the (a),(b) 894, (c),(d) 1129, and (e), (f) 1051 keV transitions. The left and right columns correspond to the 135° and 90° detectors, respectively. Red line, Doppler broadened line shape of the analyzed transition; green line, the contamination peaks; black line, the result of fitting to the experimental data.

TABLE I. The level lifetimes measured in this Letter and (average value of) level lifetimes reported in the previous works [51–53].

	Band 1		Band 2	Band 3
	τ (ps)	τ (ps)	τ (ps)	τ (ps)
I^{π} [$\hbar$]	This Letter	Previous works	This Letter	This Letter
6^+		$51^{+5\mathrm{a}}_{-5}$		
7^+		$14^{+2\mathrm{a}}_{-2}$		$1.79^{+0.14}_{-0.13}$
8^+		$32^{+3\mathrm{a}}_{-3}$	$0.62^{+0.06}_{-0.06}$	$1.21^{+0.18}_{-0.18}$
9^+		$2.4^{+0.5\mathrm{a}}_{-0.5}$	$0.53^{+0.11}_{-0.11}$	$1.10^{+0.24}_{-0.18}$
10^+	$1.32^{+0.13}_{-0.13}$	$1.19^{+0.14\mathrm{b}}_{-0.14}$	$0.43^{+0.04}_{-0.04}$	$0.38^{+0.10}_{-0.09}$
11^+	$0.42^{+0.04}_{-0.04}$	$0.46^{+0.05\mathrm{c}}_{-0.05}$	$0.25^{+0.03}_{-0.03}$	<0.60
12^+	$0.19^{+0.03}_{-0.03}$	$0.22^{+0.05\mathrm{c}}_{-0.05}$	$0.10^{+0.06}_{-0.03}$	
13^+	$0.21^{+0.02}_{-0.02}$	$0.20^{+0.04\mathrm{c}}_{-0.04}$	<0.56	
14^+	$0.14^{+0.03}_{-0.03}$	$0.15^{+0.02\mathrm{c}}_{-0.02}$	<0.29	
15^+	$0.08^{+0.01}_{-0.01}$	$0.08^{+0.03\mathrm{c}}_{-0.03}$		
16^+	<0.06	$<0.20^{\mathrm{d}}$		
17^+	<0.23	$<0.18^{\mathrm{d}}$		

[a] Average value of lifetimes in Refs. [51,52].
[b] Lifetimes in Ref. [51].
[c] Average value of lifetimes in Refs. [51,53].
[d] Lifetimes in Ref. [53].

respectively. Based on the above discussion, chirality and the wobbling mode could coexist in ^{74}Br.

To further understand the exotic rotation mode in ^{74}Br, we have carried out calculations in the framework of the quantum PRM with the pairing gap $\Delta = 12/\sqrt{A}$ MeV [62–65]. The $g_{9/2}$ proton and neutron are described by a single-j shell Hamiltonian. In the calculations, the deformation parameters $(\beta_2, \gamma) = (0.45, 27.5°)$ were used following the prediction of relativistic mean-field calculations [66]. Moreover, the moments of inertia of three axes $\mathcal{J}_{i,s,l} = 10.5$, 4.1, and 1.9 $\hbar^2$/MeV were adopted to obtain the best agreement with the experimental data, where i, s, and l stand for intermediate, short, and long axes, respectively. The present ratios of moments of inertia are close to those of the hydrodynamical moments of inertia for $\gamma = 27.5°$. The calculated results, shown in the right column of Fig. 6, reproduce the corresponding experimental data well.

The root-mean-square angular momentum components of $\boldsymbol{R}$ along the i, s, and l axes are calculated and displayed in Fig. 7. The difference between the chiral and wobbling modes is mainly reflected in their directions of core angular momentum. As shown in Fig. 7, bands 1 and 2 have similar R_i, R_s, and R_l, which agrees with the chiral picture. The R_i values of band 3 are about $1\hbar$ smaller than those of band 1 in the higher-spin range, which indicates that the core rotation of band 3 is partially transferred to the other two principal axes [2,32]. The rotational picture suggests that band 3 is the one-phonon wobbling band built on band 1. Therefore, the present theoretical calculations support the chiral interpretation for bands 1 and 2 and the wobbling excitation for band 3.

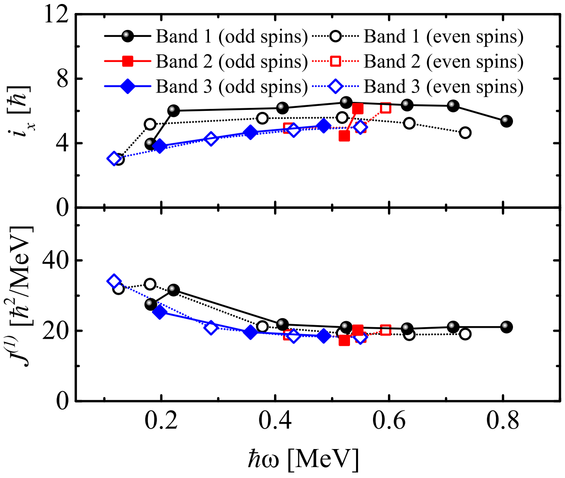

FIG. 5. Particle alignment i_x and kinematic moments of inertia $J^{(1)}$ of bands 1, 2 and 3 of ^{74}Br. The used Harris parameters are $J_0 = 6$ MeV^{-1}, $J_1 = 15$ MeV^{-3}.

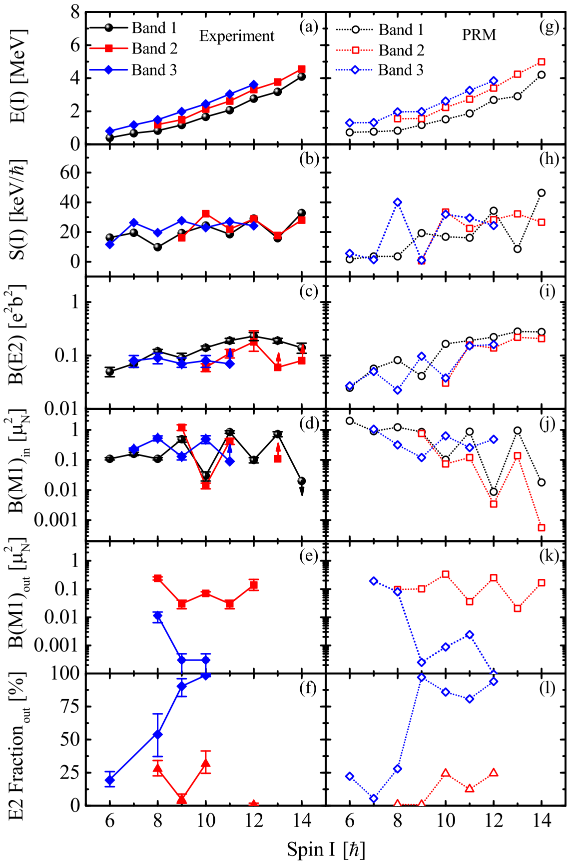

FIG. 6. Experimental (a)–(f) and calculated (g)–(l) excitation energies $E(I)$, energy staggering parameters $S(I) = [E(I) - E(I-1)]/2I$ and absolute transition probabilities $B(E2)$ and $B(M1)$ for bands 1, 2, and 3, as well as $B(M1)$ and $E2$ fraction of interband $\Delta I = 1$ transitions between bands 1, 2 and 1, 3.

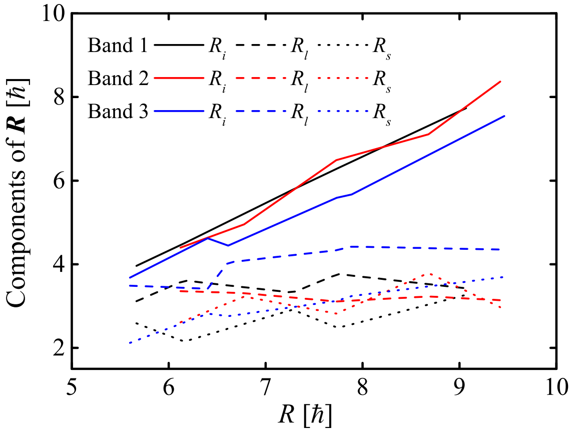

FIG. 7. Root-mean-square angular momentum components along the intermediate (i), long (l), and short (s) axes of the core angular momentum $\boldsymbol{R}$ as a function of R (calculated as $\sqrt{R_i^2 + R_s^2 + R_l^2}$) for bands 1 (black lines), 2 (red lines), and 3 (blue lines).

In summary, three $\Delta I = 1$ bands with the $\pi g_{9/2} \otimes \nu g_{9/2}$ configuration have been identified in odd-odd ^{74}Br. By comparing the experimental observations with the fingerprints of chirality and wobbling as well as PRM calculations, the second and third lowest bands have been, respectively, interpreted as the chiral partner and one-phonon wobbling excitation built on the yrast band. The observed chiral wobbler indicates that nuclear chirality can be robust against wobbling excitation. Simultaneously, the existence of the wobbling mode was extended to the $A \approx 80$ mass region and odd-odd nucleus for the first time. This finding provides a unique candidate to study chirality and the wobbling mode in a single nucleus, which manifests the diversity and complexity of the angular momentum coupling modes of nuclei. The present study opens a new arena to investigate the fundamental symmetry breaking in the $A \approx 80$ mass region and more examples in experiment of this excitation mode are expected in other mass regions. We will further investigate this chiral-wobbling nucleus experimentally, such as with a thin target experiment and g-factor measurement in the future.

We thank Professor U. Garg and Professor A. D. Ayangeakaa for providing the DSAM analysis code, professors J. Timár and S. Guo for useful discussions about the mixing ratio extractions, and iThemba LABS for technical support during this experiment. This work is partly supported by the National Natural Science Foundation of China (No. 12225504, No. 12075137, No. 12075138), the Major Program of Natural Science Foundation of Shandong Province (No. ZR2020ZD30), the Young Scholars Program of Shandong University, Weihai, and the National Research Foundation of South Africa (No. 80977). The numerical calculations in this Letter have been done on the supercomputing system in the Supercomputing Center and an HP Proliant DL785G6 server hosted by the Institute of Space Science at Shandong University, Weihai.

---

[*] sywang@sdu.edu.cn

[1] K. Starosta, T. Koike, C. J. Chiara, D. B. Fossan, D. R. LaFosse, A. A. Hecht, C. W. Beausang, M. A. Caprio, J. R. Cooper, R. Krücken *et al.*, Phys. Rev. Lett. **86**, 971 (2001).
[2] S. Ødegård, G. B. Hagemann, D. R. Jensen, M. Bergstrøm, B. Herskind, G. Sletten, S. Törmänen, J. N. Wilson, P. O. Tjøm, I. Hamamoto *et al.*, Phys. Rev. Lett. **86**, 5866 (2001).
[3] S. Frauendorf and J. Meng, Nucl. Phys. **A617**, 131 (1997).
[4] T. Koike, K. Starosta, C. Vaman, T. Ahn, D. B. Fossan, R. M. Clark, M. Cromaz, I. Y. Lee, and A. O. Macchiavelli, in Frontiers of Nuclear Structure, edited by P. Fallon and R. Clark, *AIP Conference Proceedings No. 656* (AIP, Melville, New York, 2003), p. 160.
[5] T. Koike, K. Starosta, and I. Hamamoto, Phys. Rev. Lett. **93**, 172502 (2004).

[6] S. Y. Wang, S. Q. Zhang, B. Qi, and J. Meng, Chin. Phys. Lett. **24**, 664 (2007).

[7] J. Meng and S. Q. Zhang, J. Phys. G **37**, 064025 (2010).

[8] A. Bohr and B. R. Mottelson, *Nuclear Structure* (W. A. Benjamin, New York, 1975), Vol. II, Chap. 4.

[9] H. Amro, W. C. Ma, G. B. Hagemann, R. M. Diamond, J. Domscheit, P. Fallond, A. Görgen, B. Herskind, H. Hübel, D. R. Jensen *et al.*, Phys. Lett. B **553**, 197 (2003).

[10] Ikuko Hamamoto, Phys. Rev. C **65**, 044305 (2002).

[11] A. Görgen, R. M. Clark, M. Cromaz, P. Fallon, G. B. Hagemann, H. Hübel, I. Y. Lee, A. O. Macchiavelli, G. Sletten, D. Ward *et al.*, Phys. Rev. C **69**, 031301(R) (2004).

[12] S. Frauendorf, Rev. Mod. Phys. **73**, 463 (2001).

[13] J. Meng, B. Qi, S. Q. Zhang, and S. Y. Wang, Mod. Phys. Lett. A **23**, 2560 (2008).

[14] R. A. Bark, E. O. Lieder, R. M. Lieder, E. A. Lawrie, J. J. Lawrie, S. P. Bvumbi, N. Y. Kheswa, S. S. Ntshangase, T. E. Madiba, P. L. Masiteng *et al.*, Int. J. Mod. Phys. E **23**, 1461001 (2014).

[15] J. Meng and P. W. Zhao, Phys. Scr. **91**, 053008 (2016).

[16] A. A. Raduta, Prog. Part. Nucl. Phys. **90**, 241 (2016).

[17] K. Starosta and T. Koike, Prog. Part. Nucl. Phys. **92**, 093002 (2017).

[18] B. W. Xiong and Y. Y. Wang, At. Data Nucl. Data Tables **125**, 193 (2019).

[19] S. Y. Wang, Chin. Phys. C **40**, 112001 (2020).

[20] Y. X. Luo, A. V. Ramayya, J. H. Hamilton, J. O. Rasmussen, S. J. Zhu, S. Frauendorf, J. K. Hwang, E. H. Wang, G. M. Ter-Akopian, Yu. Ts. Oganessian *et al.*, Nucl. Phys. **A919**, 67 (2013).

[21] J. Timár, Q. B. Chen, B. Kruzsicz, D. Sohler, I. Kuti, S. Q. Zhang, J. Meng, P. Joshi, R. Wadsworth, K. Starosta *et al.*, Phys. Rev. Lett. **122**, 062501 (2019).

[22] J. T. Matta, U. Garg, W. Li, S. Frauendorf, A. D. Ayangeakaa, D. Patel, K. W. Schlax, R. Palit, S. Saha, J. Sethi *et al.*, Phys. Rev. Lett. **114**, 082501 (2015).

[23] N. Sensharma, U. Garg, S. Zhu, A. D. Ayangeakaa, S. Frauendorf, W. Li, G. H. Bhat, J. A. Sheikh, M. P. Carpenter, Q. B. Chen *et al.*, Phys. Lett. B **792**, 170 (2019).

[24] Q. B. Chen, S. Frauendorf, and C. M. Petrache, Phys. Rev. C **100**, 061301(R) (2019).

[25] S. Biswas, R. Palit, S. Frauendorf, U. Garg, W. Li, G. H. Bhat, J. A. Sheikh, J. Sethi, S. Saha, Purnima Singh *et al.*, Eur. Phys. J. A **55**, 159 (2019).

[26] S. Chakraborty, H. P. Sharma, S. S. Tiwary, C. Majumder, A. K. Gupta, P. Banerjee, S. Ganguly, S. Rai, Pragati, Mayank *et al.*, Phys. Lett. B **811**, 135854 (2020).

[27] K. Rojeeta Devia, Suresh Kumar, Naveen Kumar, Neelam, F. S. Babra, Md. S. R. Laskar, S. Biswas, S. Saha, P. Singh, S. Samanta *et al.*, Phys. Lett. B **823**, 136756 (2021).

[28] D. R. Jensen, G. B. Hagemann, I. Hamamoto, S. W. Ødegård, B. Herskind, G. Sletten, J. N. Wilson, K. Spohr, H. Hübel, P. Bringel *et al.*, Phys. Rev. Lett. **89**, 142503 (2002).

[29] G. Schönwaßer, H. Hübel, G. B. Hagemann, P. Bednarczyk, G. Benzoni, A. Bracco, P. Bringel, R. Chapman, D. Curien, J. Domscheit *et al.*, Phys. Rev. B **552**, 9 (2003).

[30] P. Bringel, G. B. Hagemann, H. Hübel, A. Al-khatib, P. Bednarczyk, A. Bürger, D. Curien, G. Gangopadhyay, B. Herskind, D. R. Jensen *et al.*, Eur. Phys. J. A **24**, 167 (2005).

[31] D. J. Hartley, R. V. F. Janssens, L. L. Riedinger, M. A. Riley, A. Aguilar, M. P. Carpenter, C. J. Chiara, P. Chowdhury, I. G. Darby, U. Garg *et al.*, Phys. Rev. C **80**, 041304(R) (2009).

[32] N. Sensharma, U. Garg, Q. B. Chen, S. Frauendorf, D. P. Burdette, J. L. Cozzi, K. B. Howard, S. Zhu, M. P. Carpenter, P. Copp, F. G. Kondev *et al.*, Phys. Rev. Lett. **124**, 052501 (2020).

[33] S. Nandi, G. Mukherjee, Q. B. Chen, S. Frauendorf, R. Banik, Soumik Bhattacharya, Shabir Dar, S. Bhattacharyya, C. Bhattacharya, S. Chatterjee *et al.*, Phys. Rev. Lett. **125**, 132501 (2020).

[34] T. Koike, K. Starosta, I. Hamamoto, D. B. Fossan, and C. Vaman, AIP Conf. Proc. **764**, 87 (2005).

[35] H. Jia, S. Y. Wang, B. Qi, C. Liu, and L. Zhu, Phys. Lett. B **833**, 137303 (2022).

[36] R. A. Bark, M. Lipoglavsek, S. M. Maliage, S. S. Ntshangase, and A. Shevchenko, J. Phys. G **31**, S1747 (2005).

[37] R. T. Newman, J. J. Lawrie, B. R. S. Babu, M. S. Fetea, S. V. Förtsch, S. Naguleswaran, J. V. Pilcher, D. A. Raavé, C. Rigollet, J. F. Sharpey *et al.*, Balkan Phys. Lett., Special Issue, 182 (1998).

[38] M. Piiparinen, A. Atac, J. Blomqvist, G. B. Hagemann, B. Herskind, R. Julin, S. Juutinen, A. Lampinen, J. Nyberg, G. Sletten *et al.*, Nucl. Phys. **A605**, 191 (1996).

[39] P. M. Jones, L. Wei, F. A. Beck, P. A. Butler, T. Byrski, G. Duchêne, G. de France, F. Hannachi, G. D. Jones, and B. Kharraja, Nucl. Instrum. Methods Phys. Res., Sect. A **362**, 556 (1995).

[40] G. Duchêne, F. A. Beck, P. J. Twin, G. de France, D. Curien, L. Han, C. W. Beausang, M. A. Bentley, P. J. Nolan, and J. Simpson *et al.*, Nucl. Instrum. Methods Phys. Res., Sect. A **432**, 90 (1999).

[41] Takayoshi Aoki, Kohei Furuno, Yoshihiro Tagishi, Susumu Ohya, and J. Z. Ruan, At. Data Nucl. Data Tables **23**, 349 (1979).

[42] E. Der. Mateosian and A. W. Sunyar, At. Data Nucl. Data Tables **13**, 407 (1974).

[43] E. Macias, W. D. Ruhter, D. C. Camp, and R. G. Lanier *et al.*, Comput. Phys. Commun. **11**, 75 (1976).

[44] J. Bron, W. H. A. Hesselink, A. Van Poelgeest, J. J. A. Zalmstra, M. J. Uitzinger, H. Verheul, K. Heyde, M. Waroquier, H. Vincx, and P. Van Isacker *et al.*, Nucl. Phys. **A318**, 335 (1979).

[45] J. Döring, J. W. Holcomb, T. D. Johnson, M. A. Riley, S. L. Tabor, P. C. Womble, and G. Winter, Phys. Rev. C **47**, 2560 (1993).

[46] C. Ekström and L. Robertsson, Phys. Scr. C **22**, 344 (1980).

[47] A. D. Ayangeakaa, U. Garg, M. A. Caprio, M. P. Carpenter, S. S. Ghugre, R. V. F. Janssens, F. G. Kondev, J. T. Matta, S. Mukhopadhyay, D. Patel *et al.*, Phys. Rev. Lett. **110**, 102501 (2013).

[48] J. Ziegler, *Stopping and Ranges of Ions in Matter* (Pergamon Press, New York, 1980), Vols. 3 and 5.

[49] C. J. Chiara, S. J. Asztalos, B. Busse, R. M. Clark, M. Cromaz, M. A. Deleplanque, R. M. Diamond, P. Fallon,

D. B. Fossan, D. G. Jenkins *et al.*, Phys. Rev. C **61**, 034318 (2000).
[50] C. J. Chiara, D. B. Fossan, V. P. Janzen, T. Koike, D. R. LaFosse, G. J. Lane, S. M. Mullins, E. S. Paul, D. C. Radford, H. Schnare *et al.*, Phys. Rev. C **64**, 054314 (2001).
[51] J. W. Holcomb, T. D. Johnson, P. C. Womble, P. D. Cottle, S. L. Tabor, F. E. Durham, and S. G. Buccino, Phys. Rev. C **43**, 470 (1991).
[52] G. García-Bermúdez, M. A. Cardona, A. Filevich, R. V. Ribas, H. Somacal, and L. Szybisz, Phys. Rev. C **59**, 1999 (1998).
[53] R. Loritz, O. Iordanov, E. Galindo, A. Jungclaus, D. Kast, K. P. Lieb, C. Teich, F. Cristancho, Ch. Ender, T. Häartlein *et al.*, Eur. Phys. J. A **6**, 257 (1999).
[54] G. Winter, J. Döring, W. D. Fromm, L. Funke, P. Kemnitz, and E. Will, Z. Phys. A **309**, 243 (1983).
[55] T. Koike, K. Starosta, C. J. Chiara, D. B. Fossan, and D. R. LaFosse, Phys. Rev. C **63**, 061304(R) (2001).
[56] G. Rainovski, E. S. Paul, H. J. Chantler, P. J. Nolan, D. G. Jenkins, R. Wadsworth, P. Raddon, A. Simons, D. B. Fossan, T. Koike *et al.*, Phys. Rev. C **68**, 024318 (2003).
[57] S. Y. Wang, B. Qi, L. Liu, S. Q. Zhang, H. Hua, X. Q. Li, Y. Y. Chen, L. H. Zhu, J. Meng, S. M. Wyngaardt *et al.*, Phys. Lett. B **703**, 40 (2011).
[58] C. Liu, S. Y. Wang, R. A. Bark, S. Q. Zhang, J. Meng, B. Qi, P. Jones, S. M. Wyngaardt, J. Zhao, C. Xu *et al.*, Phys. Rev. Lett. **116**, 112501 (2016).
[59] C. Liu, S. Y. Wang, B. Qi, S. Wang, D. P. Sun, Z. Q. Li, R. A. Bark, P. Jones, J. J. Lawrie, L. Masebi *et al.*, Phys. Rev. C **100**, 054309 (2019).
[60] W. Z. Xu, S. Y. Wang, C. Liu, X. G. Wu, R. J. Guo, B. Qi, J. Zhao, A. Rohilla, H. Jia, G. S. Li *et al.*, Phys. Lett. B **833**, 137287 (2022).
[61] See Supplemental Material at http://link.aps.org/supplemental/10.1103/PhysRevLett.132.092501 for table of the measured intensity, ADO ratio, linear polarization, mixing ratio, $E2$ fraction, and $B(M1)$ and $B(E2)$ of transitions.
[62] S. Q. Zhang, B. Qi, S. Y. Wang, and J. Meng, Phys. Rev. C **75**, 044307 (2007).
[63] S. Y. Wang, S. Q. Zhang, B. Qi, and J. Meng, Phys. Rev. C **75**, 024309 (2007).
[64] S. Y. Wang, S. Q. Zhang, B. Qi, J. Peng, J. M. Yao, and J. Meng, Phys. Rev. C **77**, 034314 (2008).
[65] S. Y. Wang, B. Qi, and D. P. Sun, Phys. Rev. C **82**, 027303 (2010).
[66] B. Qi, H. Jia, C. Liu, and S. Y. Wang, Sci. China **62**, 012012 (2019).